ORIGINAL PAPER

The *Acanthamoeba* Shikimate Pathway has a Unique Molecular Arrangement and is Essential for Aromatic Amino Acid Biosynthesis

Fiona L. Henriquez[a], Sara J. Campbell[a,b], Bharath K. Sundararaj[a,b], Antonella Cano[b], Stephen P. Muench[c], and Craig W. Roberts[b,1]

[a]Institute of Biomedical Science and Environmental Health Research, School of Science, University of the West of Scotland, Paisley, PA1 2BE, UK

[b]Strathclyde Institute of Pharmacy and Biomedical Sciences, University of Strathclyde, 161 Cathedral Street, Glasgow, G4 0NR, UK

[c]School of Biomedical Sciences, University of Leeds, Leeds, LS2 9JT

Running title: *Acanthamoeba* Shikimate Pathway

[1]Corresponding author; e-mail c.w.roberts@strath.ac.uk (C. W. Roberts).

The shikimate pathway is the only known biosynthetic route for de novo synthesis of aromatic compounds. It is described as an ancient eukaryotic innovation that has been retained in a subset of eukaryotes, replaced in plants through the acquisition of the chloroplast, but lost in many including humans. Herein, we demonstrate that *Acanthamoeba castellanii* possesses the shikimate pathway by biochemical and a combination of bioinformatics and molecular biological methods. The growth of *A. castellanii* (Neff strain and a recently isolated clinical specimen, both T4 genotypes) is inhibited by glyphosate [N-(phosphonomethyl) glycine], an inhibitor of EPSP synthase and the addition of phenylalanine and tryptophan, which are dependent on the shikimate pathway, rescued *A. castellanii* from glyphosate indicating that glyphosate was specific in action. *A. castellanii* has a novel complement of shikimate pathway enzymes including unique gene fusions, two Type I and one Type II DAHP synthases (for which their likely sensitivities to feedback inhibition by phenylalanine, tyrosine and tryptophan has been modelled) and a canonical chorismate synthase. The shikimate pathway in *A. castellanii* therefore has a novel molecular arrangement, is required for amino acid biosynthesis and represents an attractive target for antimicrobials.

Key words: *Acanthamoeba castellanii*; shikimate pathway; glyphosate inihibition; novel molecular arrangement.

Introduction

Acanthamoeba (species) are facultative parasites that can cause a painful sight-threatening keratitis or fatal granulomatous encephalitis in humans. Although many options for the treatment of ocular *Acanthamoeba* infections exist, most are essentially disinfectants that have necessarily arduous regimens with limited efficacy (Marciano-Cabral and Cabral 2003).   Furthermore, eye care solutions are not currently routinely tested against *Acanthamoeba* and no single-step contact lens solution has proven effective at decontaminating lenses from *Acanthamoeba*. Granulomatous Amoebic Encephalitis (GAE) is normally associated with immunosuppression and is almost always fatal as current treatments are generally ineffective (Seijo Martinez et al. 2000). Identification and exploitation of new antimicrobial targets against *Acanthamoeba* is therefore desirable.

The shikimate pathway is a promising target for antimicrobial design since it is the only known route for de novo synthesis of aromatic compounds. The shikimate pathway was once thought to be restricted to prokaryotes, plants (where it is associated with the chloroplast) and fungi. It has more recently been demonstrated to be present in some chromalveolates including the medically important apicomplexans *Toxoplasma gondii and Plasmodium* species*,* at least some ciliates and the agriculturally important oomycete, *Phytophthora ramorum* (Richards et al. 2006; Roberts et al. 1998). The pathway is now known to be present in phylogenetically divergent extant eukaryotic taxa and it has been proposed that it was therefore present in their last common ancestor (Campbell et al. 2004; Richards et al. 2006). Some additional weight to this is given by the molecular arrangement of the enzymes responsible and their phylogeny. Thus with the exception of phototrophic organisms that have a chloroplast-located, prokaryotic derived pathway, all eukaryotes examined to date have a characteristic pentafunctional gene fusion (arom) encoding a single polypeptide responsible for 5 (3-dehydroquinate synthase, 3-dehydroquinate dehydratase, shikimate 5-dehydrogenase, shikimate kinase and EPSP synthase) out of the seven enzyme activities (Richards et al. 2006). Phylogenetic studies support that this molecular arrangement is an ancient eukaryotic innovation that has been inherited in diverse eukaryotes through vertical decent

72 (Richards et al. 2006). In contrast, bacterial shikimate pathway enzymes are encoded on individual

73 polypeptides (Roberts et al. 1998). This arrangement is conserved in plants with the exception of 3-

74 dehydroquinate dehydratase and shikimate 5-dehydrogenase, which form a bifunctional protein

75 (Campbell et al. 2004). In addition, two non-homologous types of DAHP synthase (designated

76 class I and II) have been found across a variety of organisms (Butler et al. 1974). Class I proteins

77 (often occurring as multiple paralogs in a single organism) were originally identified in prokaryotes,

78 but are also found in many fungi and the chromalveolates, *Phytophthora ramorum* and

79 *Phytophthora infestans* (Coggins et al. 1987; Herrmann and Weaver 1999; Richards et al 2006).

80 Although class II DAHP synthases were first identified in plants, they are now known to be in

81 bacteria, fungi and the chromalveolate *Toxoplasma gondii* (Dyer et al. 1990; Gosset et al. 2001;

82 Richards et al. 2006; Shumilin et al. 1996). A number of prokaryotes and some fungi including

83 *Neurospora crassa* contain both classes of DAHP synthases (Walker et al. 1996). Class I DAHP

84 synthases often existing as multiple paralogs and class II DAHP synthases are frequently regulated

85 by one or more aromatic amino acids (Jensen et al. 2002).

86 The shikimate pathway is still relatively rare in sampled eukaryotes and is absent in

87 mammals that acquire their aromatic compounds from diet. This makes it an attractive target for

88 antimicrobial agents (Bentley 1990; Jensen 1996; Roberts et al. 2002). Herein, we demonstrate that

89 the shikimate pathway is essential for *Acanthamoeba* growth in absence of exogenous aromatic

90 amino acids, describe its molecular organisation and demonstrate its potential as a target for

91 antimicrobials.

92

Results

94 **Glyphosate Restricts *Acanthamoeba castellanii* Growth in vitro**

95 The effectiveness of glyphosate as an inhibitor of *A. castellanii* growth was assessed by a modified

96 version of the alamarBlue microtiter plate assay. *A. castellanii* trophozoites were grown in defined

medium lacking aromatic compounds (folate and the aromatic amino acids tyrosine, phenylalanine and tryptophan). Glyphosate significantly restricted *A. castellanii* Neff strain and the *A. castellanii* clinical strain growth in a dose dependent manner (Fig. 1). The IC_{50} for the Neff strain was determined to be between 17.5μM and 35μM for the Neff strain and 70μM to 140μM for the clinical strain. Importantly, it did not induce encystment (Fig. 1D).

Glyphosate is not Toxic to Rabbit Corneal Epithelial Cells

The toxicity of glyphosate to rabbit corneal epithelial (RCE) cells was assessed via the alamarblue microtiter plate assay. There was no inhibition of the metabolic activity of the RCE by glyphosate at concentrations (17.5μM to 1130μM), which inhibited the growth of *A. castellanii* (Fig. 1C).

***Acanthamoeba* Relies on the Shikimate Pathway for Aromatic Amino Acids**

To confirm that glyphosate was specifically acting on EPSP synthase and thus the shikimate pathway and to determine which products derived from the shikimate pathway, precursors were necessary for *A. castellanii*, PABA and aromatic amino acids were added alone and in combination to glyphosate treated trophozoites. The addition of tyrosine (up to 0.66mM), phenylalanine (up to 10mM) and tryptophan (up to 1.96mM) separately did not negate the effects of glyphosate (Fig. 2A). However, simultaneous addition of phenylalanine and tryptophan ablated any inhibitory effect of glyphosate (Fig. 2B). Tyrosine, in combination with either phenylalanine or tryptophan, and PABA were neither necessary nor sufficient to ablate glyphosate inhibition (Fig. 2B, C). Bioinformatic analyses have identified all enzymes necessary for the production of phenylalanine (Fig. 3), tryptophan and folates from chorismate (Supplementary Material Fig. S1). Enzymes involved in tyrosine biosynthesis directly from chorismate are not present, but those necessary for

5

120 tyrosine biosynthesis from phenylalanine via phenylalanine-4-hydroxylase are present (Genbank

121 ELR14932.1). Notably, the enzymes involved in ubiquinone biosynthesis are not found.

122

Acanthamoeba have both Type I and II DAHP Synthases

124 The transcriptome data (Clarke et al. 2013) was interrogated and two type I DAHP synthases

125 (DAHPI) were identified.(Accession numbers ELR16577.1 and ELR11971.1). Both DAHP

126 synthases were successfully amplified from *A. castellanii* Neff strain and clinical specimen cDNAs

127 (Accession numbers KC471625 and KC471626, respectively, Fig. 4A).

128 The Phyre2 program produced models for each enzyme and permitted an examination of the

129 Phe/Tyr/Trp inhibition site conservation for AcDAHPIa and AcDAHPIb. A model for the type I

130 DAHP synthase was generated from both *A.castellanii* sequences based on the *E. coli* crystal

131 structure to which both sequences share very high sequence identity (Fig. 4A). The Phe binding

132 pocket is formed by 16 residues, of which only 1 differs in the *E. coli* structure with Ser being

133 replaced by Gly in the AcDAHPIa, but not AcDAHPIb sequence (Fig. 4A). The predicted position

134 of Ser allows it to pack against the the Phe substrate with the replacement by Gly in the AcDAHPIa

135 sequence possibly accommodation of the bulkier hydroxyl group of a Tyr residue (Fig. 4C, D). This

136 Ser/Gly change may allow for the type I DAHP synthase to be regulated by Tyr or Phe in the

137 AcDAHPIa and AcDAHPIb sequences, respectively.

138 DAHP synthase type II (DAHPII) was found in the *A. castellanii* transcriptome (Accession

139 number ELR24167) (Clark et al. 2013). The putative *A. castellanii* DAHPII shares a high degree of

140 similarity to a number of type II DAHP synthases. Modelling of the *A. castellanii* DAHP type II

141 (AcDAHPII) synthase was based on *M. tuberculosis* DAHP typeII (MtDAHPII), which has been

142 solved in complex with both Phe and Trp inhibitors (Webby et al. 2010). The MtDAHPII contains a

143 primary Phe binding site located in the heart of the dimer interface, formed by residues from each

144 monomer. Of the 10 residues which make up the binding pocket only 2 are conserved with a further

2 showing close similarity (Fig. 5A), with 2 residues found on the C-terminal β-strand which is predicted to be structurally absent in the AcDAHPII structure (Fig. 4A). Moreover, those residues responsible for forming a hydrogen bond network in MtDAHPII (Arg171 and Asn175) are replaced by Gln and His, respectively (Fig. 5B). The replacement of Ala in MtDAHPII to Phe in AcDAHPII in the predicted Phe binding site, may also create a steric clashes and would make dimer formation in the presence of Phe unlikely (Fig. 5C). The secondary Phe binding site within MtDAHPII involves 9 residues of which Arg23, Arg256 and Glu53 have been shown to be critical in forming a hydrogen bond network to the α-carboxylate group of the Phe inhibitor, none of these are conserved in AcDAHPII but are replaced by Thr, Ala and Gln, respectively. This significant change would make it unlikely that the AcDAHPII enzyme is inhibited by Phe in a manner similar to that seen for MtDAHPII. In addition to Phe, MtDAHPII is also inhibited by Trp which binds in a site formed by 17 residues of which 6 are identical and 4 are similar in the AcDAHPII enzyme. Modelling suggests that AcDAHPII would have a similar hydrophobic binding pocket of the same approximate shape. Interestingly, MtDAHPII is inhibited only by the presence of both Phe/Tyr and Trp at biologically relevant concentrations. The predicted lack of a conserved Phe/Tyr binding site may imply that AcDAHPII is inhibited only by Trp and does not require the allosteric binding of Phe or Tyr. Alternatively Trp does not regulate the enzyme, or an alternative binding site is present which has so far not been characterised. Further biochemical and structural investigation is required to validate these models which give only a prediction of the *A. castellanii* DAHP family.

Acanthamoeba have a Novel Tetrafunctional Protein with Tetrafunctional Gene Fusion Comprising 3-dehydroquinate Synthase (DHQS), 5-enolpyruvylshikimate-3-phosphate Synthase (EPSPS), Shikimate Kinase (SK) and 3-dehydroquinate Dehydratase (DH)

Bioinformatical analysis of the transcriptome data (Clarke et al. 2013) reveals that four out of five of the AROM enzymes are present in a tetrameric fusion and that the shikimate dehydrogenase is

missing from the sequence. Accession number ELR24870 is named shikimate kinase but it actually contains 3-hydroquinate synthase (DHQS), 5-enolpyruvylshikimate-3-phosphate synthase (EPSPS), shikimate kinase (SK) and 3-dehydroquinate dehydratase (DH). This unusual and novel arrangement was confirmed by PCR from cDNA from both *A. castellanii* Neff strain and the clinical strain (KC479580 and KC471623, respectively; Fig. 6). The AROM-like sequence (aromN –Novel-) is 3927 nucleotides in length, and codes for protein with a predicted molecular weight of 143.3kDa and shares identity and similarity with a number of AROM proteins from other species (Supplementary Material Fig. S2).

Acanthamoeba castellanii have a Novel Trifunctional Gene Fusion Comprising Shikimate Dehydrogenase, Phosphoribosylanthranilate Isomerase and Indole-3-glycerol-phosphate Synthase

Analysis of the transcriptome data (Clarke et al. 2013) confirmed the existence of a novel trifunctional gene fusion comprising of indole-3-glycerol-phosphate synthase, phosphoribosylanthranilate isomerase and shikimate dehydrogenase (Accession number ELR21144). This fusion was confirmed by PCR in both strains studied (Accession numbers KC479581 and KC471624, Neff and clinical isolates, respectively; Supplementary Material Fig. S3). Modelling of the trimeric fusion proved unreliable due to the absence of a current complex structure. However, two models could be reliably generated of the bi-functional 2 phosphoribosylanthranilate isomerase:3 indoleglycerolphosphate (RCSB ID. 1pii) and bi-functional 3–dehydroquinate dehydratase/shikimate dehydrogenase (RCSB ID 2o7q). The common fold shared between the bi-functional complexes and their subsequent superposition permits for an approximate model of the trimeric fusion to be generated.

***Acanthamoeba* have a Canonical Chorismate Synthase**

Based on these sequences primers (chorismate synthase For 5'-GGTGCAGGCGACAAGGCAAC-3' and chorismate synthase REV 5'-AAGTACTTTTTCTGGAGCTG-3') were designed and hot start, which spans both contigs identified. *A. castellanii* chorismate synthase is present in the transcriptome (Accession number ELR21143) (Clarke et al. 2013). PCR (annealing at 58 ^{o}C) amplified the gene encoding chorismate synthase from *A. castellanii Neff* strain cDNA (Accession number KC471628) and subsequently from the clinical isolate (Accession number KC471627). AcCS shares identity and similarity with a number of type I chorismate synthases from other species (Supplementary Material Fig. S4).

Discussion

Our work has demonstrated that the shikimate pathway has a wider eukaryotic phylogenetic distribution than previously thought (Campbell et al. 2004; Richards et al. 2006). Thus, the shikimate pathway would appear to have been present in the last universal common ancestor of eukaryotes and has been selectively lost in the vast majority of extant eukaryotes sampled to date, replaced in plants predominantly through the acquisition of the chloroplast and retained by fungi, and a select few of sampled chromalveolates including some apicomplexans, ciliates and oomycetes (Campbell et al. 2004; Richards et al. 2006). The current studies now demonstrate the shikimate pathway in at least one member of the Amoebozoa. This would support the notion that the shikimate pathway is an ancient eukaryotic trait. The ability of glyphosate to inhibit the growth of a laboratory strain of *A. castellanii* (Neff) and a recently isolated clinical strain demonstrates the potential utility of targeting this pathway with antimicrobials.

The shikimate pathway catalyses the sequential conversion of erythrose 4–phosphate and phosphoenol pyruvate to chorismate in seven steps. The studies described here fully characterise

and report the existence of the shikimate pathway in *A. castellanii*. The pathway has the potential to be an antimicrobial target used to limit infection and the genes encoding the enzymes of this pathway have a novel molecular arrangement.

The potential for the shikimate pathway to be an antimicrobial target is exemplified by glyphosate which restricts *A. castellanii* growth in a dose-dependent manner, albeit in the absence of the pathway's end products (aromatic amino acids, folate and ubiquinone). Interestingly, only a combination of phenylalanine and tryptophan or all three aromatic amino acids together can rescue *A. castellanii* growth from the effects of glyphosate. Bioinformatic analysis reveals that *A. castellanii* can create phenylalanine and tryptophan directly from chorismate, whereas the important enzyme, prephenate dehydrogenase in tyrosine synthesis from chorismate is not present. However, tyrosine can be synthesised from phenylalanine via the enzyme phenylalanine-4-hydroxylase. *A. castellanii* also possess the ability to synthesise folates. However, the addition of folates alone did not ablate the inhibitory effect of glyphosate. A plausible explanation to the reason that aromatic amino acids can rescue *A. castellanii* growth in the absence of folate but the reverse is not possible may be due to the fact that folates can be recycled through gammaglutamyl hydrolase (EC 3.4.19.9), which has been identified in *A. castellanii* (ELR19434) (Clarke et al. 2013). In our experiments, it is likely that *A. castellanii* are recycling folate, since they are initially maintained in a rich mycological peptone medium before a step by step passage to a defined minimal medium. Enzymes involved in ubiquinone biosynthesis have not been found despite extensive bioinformatical searches. Future studies will be required to determine how *A. castellanii* acquires ubiquinone.

We have for the first time identified two class I DAHP synthases and a class II DAHP synthase in *A. castellanii*. This is similar to the situation in *Neurospora crassa* where it has both a tyrosine sensitive and a phenylalanine sensitive class 1 DAHP synthase along with a class II DAHP synthase that is sensitive to tryptophan (Chaleff et al. 1974). Modelling of the two *A. castellanii* class I DAHP sequences has suggested the apparent conservation of the Phe binding site with the

10

244 replacement of Ser to Gly in the binding site possibly permitting the two *A. castellanii* class I

245 DAHP synthases to be regulated by both Phe and Tyr (Fig. 3), although further biochemical studies

246 are required to validate this. Unlike bacteria, which contain an AroF, AroG and AroH class I

247 DAHP synthase, which can be regulated by Tyr, Phe and Trp, respectively, *A. castellanii* has only

248 the AroG homologue. The two different AroG sequence, may allow for a Phe or Tyr regulation

249 mechanism although no clear Trp site can be identified. Further biochemical characterisation will be

250 required to show that both Tyr and Phe can regulate the shikimate pathway through the two class I

251 enzymes.

252   In addition to the class I DAHP enzymes a second class of DAHP enzyme has been found

253 which is distinct in architecture form the class I family. This second class has been shown to be

254 regulated by Phe, Tyr and Trp with either Phe/Tyr being required in the presence of Trp to cause

255 inhibition. The structure of the *M. tuberculosis* class II DAHP enzyme (MtDAHPII) has

256 characterised the architecture of both the Phe/Tyr and Trp binding pockets. Modelling of *A.*

257 *castellanii* homologues suggests it may lack the pre-requisite amino acids, which form the binding

258 site with an Ala/Phe mutation causing a severe steric clash with the proposed bound Phe. The Trp

259 binding site appears well conserved within the *A. castellanii* class II DAHP (AcDAHPII) although

260 whether this binding requires the cooperative binding of Phe/Tyr as well is as yet undetermined.

261 The putative modelling has predicted that *A. castellanii* has 3 DAHP enzymes, (2 class I and 1 class

262 II), of these the class I enzymes can be regulated by Phe/Tyr and the class II by Trp. Other binding

263 sites may exist which have not yet been characterised. However, these results show that the

264 shikimate pathway in *A. castellanii* could be feedback regulated by 3 different aromatic amino acids

265 as described in *Neurospora crassa* (Chaleff et al. 1974).

266   The shikimate pathway enzymes have distinct molecular organisations in different groups of

267 species (Chaleff et al. 1974). Each of the shikimate pathway enzymes is encoded on individual

268 polypeptides in bacteria (Butler et al. 1974). Plants have discrete polypeptides with each enzyme

269 activity with the exception of 3-dehydroquinate dehydratase and shikimate 5-dehydrogenase which

11

are fused as separate domains on a single polypeptide (Coggins et al. 1987). In all eukaryotes previously examined, 3-dehydroquinate synthase, 3-dehydroquinate dehydratase, shikimate 5-dehydrogenase, shikimate kinase and EPSP synthase are encoded on a single transcript to form a pentafunctional polypeptide (termed AROM) (Richards et al. 2006). The current studies now describe a further novel arrangement as *A. castellanii* consisting of two previously undescribed gene fusions. Thus, *A. castellanii* have a novel tetrafunctional protein comprising 3-dehydroquinate synthase, 5-enolpyruvylshikimate-3-phosphate (EPSP) synthase, 3-dehydroquinate dehydratase and shikimate kinase. This fusion has the four enzyme activities ordered in the same sequence as the first 4 activities of AROM. We have designated this tetrafunctional protein AROMn ('n' is not only next in the alphabet, but to also denotes this novel arrangement). The enzyme activity missing from the AROM-like protein, shikimate dehydrogenase is instead part of a novel trifunctional protein comprising shikimate dehydrogenase, phosphoribosylanthranilate isomerase and indole-3-glycerol-phosphate synthase. Although a gene fusion comprising shikimate dehydrogenase with these 2 tryptophan biosynthesis enzymes is novel, certain eukaryotes including *Phaeodactylum tricornutum* (a diatom), *P. ramorum* (an oomycete) and *Ustilago maydis* (a fungus) have a fused phosphoribosylanthranilate isomerase and indole-3-glycerol-phosphate synthase (Jiroutová et al. 2007). The functional implications, if any of this fusion is yet to be determined, but its unique arrangement could prove to be a novel target for therapeutic development. These novel gene fusions will require phylogenetic analyses to determine their likely evolutionary origins.

Chorismate synthase is responsible for the final reaction of the shikimate pathway and is dependent on reduced flavin for its function. Chorismate synthase is known to have an endogenous flavin reductase capability in fungi, apicomplexans and ciliates examined to date (Ehammer et al. 2007). However, in plants and bacteria chorismate synthase has been found to lack flavin reductase ability and is thus dependent on an alternative source. From chorismate a number of aromatic products are derived, including folate, ubiquinone and aromatic amino acids. All enzymes

belonging to these pathways have been identified through bioinformatical analysis (Clarke et al. 2013) (Supplementary Material Fig. S1).

The shikimate pathway has been exploited in plants as a target for herbicides (Bentley, 1990) and proposed as an antimicrobial target in a number of pathogens including bacteria, fungi and protozoans. In addition to glyphosate and number of compounds targeting EPSP synthase have been experimentally tested as antimicrobials (Bentley 1990). Other enzymes in the shikimate pathway or downstream of the shikimate pathway have been inhibited by substrate analogues. Thus for example, (6S)-6-fluoroshikimate and (6R)-6-fluoroshikimate through a process of biotransformation ultimately inhibit 4-aminobenzoic acid synthesis and chorismate synthase respectively (Bentley 1990). The work described here suggests that the current antimicrobials designed against the shikimate pathway have potential against *A. castellanii* and may provide further motivation to develop new inhibitors of this pathway. These inhibitors could be used to improve the treatment of *A. castellanii* and improve the ability of contact lens solutions to kill this potential pathogen. It is also likely that the shikimate pathway is also present in other *Acanthamoeba* species based on genetic similarities (Henriquez et al. 2008).

In conclusion we demonstrate that *A. castellanii* have a novel shikimate pathway with as yet unique gene fusions. This pathway is essential for the production of aromatic amino acids and the survival of *A. castellanii* and may be exploitable as an antimicrobial agent target.

Methods

13

Maintenance of *Acanthamoeba castellanii* trophozoites: *Acanthamoeba castellanii* (*A. castellanii*) (Neff strain) was originally obtained from Keith Vickerman (Glasgow, United Kingdom). *A. castellanii* T4 (Clinical isolate), isolated from a patient with keratitis was obtained from Antonella Mattana (University of Sassari, Italy) *A. castellanii* trophozoites were routinely grown in 2% mycological peptone w/v (Sigma, Poole, United Kingdom) and 0.9% w/v maltose (Sigma), or M11 media as previously described by Shukla *et al.*, (1990) modified by removal of aromatic compounds and augmentation of glucose levels to 36% w/v. Media were supplemented with 125µg penicillin/ streptomycin (Sigma). They were incubated until confluent at room temperature, unless otherwise stated, in 75-cm^2 tissue culture flasks when they were either subcultured or harvested following mechanically induced detachment.

Rabbit corneal epithelial cells: Rabbit corneal epithelial (RCE) cells (ECACC No. 950810146) were cultured in Dulbecco's Modified Eagle's Medium (DMEM) Ham's F-12 (1:1) containing 15mM HEPES and L-glutamine, supplemented with human corneal growth supplement (HCGS) (Life Technologies Paisley, United Kingdom), 10% heat-inactivated foetal calf serum (Sigma), 125µg penicillin/ streptomycin and 125µg amphotericin B (Sigma). RCE cells were incubated at 37 ^{o}C, 5% CO_2 in 75-cm^2 tissue culture flasks until 90-95% confluent, then harvested or sub-cultured by using TrypLE^{TM} Express enzyme cell detaching medium (Life Technologies).

***A. castellanii* trophozoite growth inhibition assays:** *A. castellanii* trophozoites were
routinely cultured as described above. Confluent flasks were subcultured by mechanical detachment
to increasing concentrations of modified M11 media (50%, 80%, 100%), supplemented with 2%
mycological peptone and 0.9% maltose and with 125μg penicillin/ streptomycin and 125μg
amphotericin B (Sigma, Poole, United Kingdom). The effectiveness of N-(phosphonomethyl)
glycine (glyphosate) as an inhibitor of *A. castellanii* trophozoites was determined by a modified
version of the colorimetric microtiter plate assay described by McBride *et al.*, (2005). *A. castellanii*
cultured in 100% modified M11 media were seeded in triplicate at a concentration of either 4 x
10^5/ml (Neff Strain) or 1 x 10^6 (Clinical isolate) in a 96 well tissue culture plate (TPP, Switzerland).
Glyphosate (Sigma) was dissolved in modified M11 media and 50μl was added to each well in
serial dilutions from 1130μM to 1.1μM. Control wells were supplemented with 50μl of modified
M11 medium. Where appropriate, aromatic amino acids and/or para-aminobenzoic acid (PABA)
were added separately at different concentrations as stated to determine if such treatment could
ablate the effects of glyphosate. The assay was then incubated for 48 hours at room temperature and
10μl of AlamarBlue reagent (Biosource, Europe) was added to each well and further incubated at
room temperature, in the dark, for 24 hours. Absorbances were then read on spectromax (Molecular
Devices) at OD_{570} and OD_{600}.

The percentage inhibition of AlamarBlue^{TM} was calculated by the following formula:

$$\{[(\varepsilon_{ox}\lambda_2)(A\,\lambda_1)] - [(\varepsilon_{ox}\lambda_1)(A\,\lambda_2)] / [(\varepsilon_{ox}\lambda_2)(A\,^o\lambda_1)] - [(\varepsilon_{ox}\lambda_1)(A\,^o\lambda_2)]\} \times 100$$

Where $\varepsilon_{ox}\lambda_1$ is 80,586 (molar extinction coefficient of oxidised AlamarBlue at 570nm); $\varepsilon_{ox}\lambda_2$ is
117,216 (molar extinction coefficient of oxidised AlamarBlue at 600nm); $A\,\lambda_1$ is the absorbance of
the treated wells at 570nm; $A\,\lambda_2$ is the absorbance of the treated wells at 600nm; $A^o\lambda_1$ is the
absorbance of the untreated control wells at 570nm; $A^o\lambda_2$ is the absorbance of the untreated control
wells at 600nm. These absorbance values were subtracted from 100 to give percentage of

357 AlamarBlue[TM] reduction in comparison to untreated controls. The results were expressed as a mean

358 for each triplicate ± the standard error (SE) and student T-test analyses were performed.

359 **Assessment of inhibitor-induced encystment:** *A. castellanii* were cultured, harvested and

360 seeded as described previously with glyphosate (Sigma) dissolved in modified M11 media and

361 incubated for 72 hrs at room temperature. Sodium dodecyl sulphate (SDS), which causes

362 immediate lysis of *A. castellanii* trophozoites while mature cysts remain intact, was then used to

363 assess if the presence of glyphosate had caused *A. castellanii* to form cysts. The medium was

364 carefully removed and replaced with 100µl of 5% SDS then cells were counted manually on a

365 haemocytometer. The effect of 5% SDS was also assessed on cyst controls. In brief 4 x 10^5/ml *A.*

366 *castellanii* were resuspended in encystment medium (20 mM Tris-HCl [pH 8.8], 100 mM KCl, 8

367 mM $MgSO_4$, 0.4 mM $CaCl_2$, 1 mM $NaHCO_3$) (Campbell et al. 2008) and incubated at room

368 temperature until cysts had formed. Cells were then resuspended in 5% SDS and counted manually

369 on a haemocytometer.

370 **Susceptibility of rabbit corneal epithelial (RCE) cells to glyphosate:** RCE were cultured

371 and harvested as described. The effect of glyphosate was determined as described by McBride et al.

372 (2007). Cells were seeded in triplicate at 280 cells per well in 50µl of RCE medium in a 96 well

373 tissue culture plate (TPP, Switzerland) and allowed to adhere for 3 hours at 37 ^{o}C, 5% CO_2.

374 Glyphosate (Sigma) was dissolved in 10ml of RCE medium and 50µl was added to each well to

375 give the final concentrations from 1130µM to 17.5µM. Control wells were supplemented with 50µl

376 of RCE medium and plates were incubated for 96 hours at 37°C, 5% CO_2. 10µl of alamarBlue

377 reagent was added to wells 6 hours prior to the end of the incubation. Absorbance was then read on

378 spectromax (Molecular Devices) at OD_{570} and OD_{600} and the percentage inhibition of alamarBlue

379 reduction was calculated as previously described.

380 **RNA extraction:** *A. castellanii* were cultured and harvested as normal from modified M11

381 medium. Cells were collected by a 5 minute centrifugation at 21000g at 4 ^{o}C and the pellet was

382 then suspended in 1.0ml of Trizol® reagent (Life Technologies). Total RNA was isolated using a

16

method based on a single-step acid guanidinium thiocyanate-phenol-chloroform protocol described

by Chomczynski & Sacchi (1987). The concentration was determined by measuring absorbance at

260 nm on a spectrophotometer (GeneQuant pro, Amersham Biosciences, and United Kingdom).

Extracted RNA was then stored at -80 ^{o}C until required for cDNA synthesis and the integrity of the

RNA was assessed via PCR and or gel electrophoresis on a 2% agarose gel.

A. castellanii **genomic DNA extraction:** Genomic DNA (gDNA) was obtained by a

modification of the method of Johnson et al. (1986). In brief, 10^7 cells were collected by 10-min

centrifugation at 7000g and 4 ^{o}C. The pellet was resuspended in 10ml of 0.2M NaCl/10mM

EDTA/10mM Tris-HCl (pH 8.0), 1% SDS, 200μg/ml Proteinase K (Sigma, Poole, United

Kingdom), and incubated 3 hours at 50 ^{o}C with gentle agitation. 10ml of

phenol/chloroform/isoamyl alcohol (50:48:2) was added before centrifugation for 10 minutes at

3000g and 4 ^{o}C. The supernatant was removed and this was repeated until the interface was clear.

The DNA solution was extracted with 10ml of chloroform and centrifugation for 10 minutes at

3000g at 4 ^{o}C before the addition of 20μg/ml of RNase A and a further incubation at 4 ^{o}C for 15

minutes. DNA was precipitated with 10M ammonium acetate and 100% ethanol at -20 ^{o}C for 1hr

followed by a 10 minute centrifugation at 10,000g and 4 ^{o}C. The pellet was resuspended in 0.5 ml

of TE buffer (10mM Tris-HCL, 1mM EDTA, pH 8.0) and the concentration determined by

measuring absorbance at 260 nm on a spectrophotometer (GeneQuant pro, Amersham Biosciences,

United Kingdom). The integrity of the DNA was assessed via gel electrophoresis on a 0.8%

agarose gel. All samples were stored at 4 ^{o}C until required.

Complementary DNA (cDNA) synthesis and Polymerase chain reaction (PCR):
Complementary DNA (cDNA) was synthesised from *A. castellanii* total RNA, using AffinityScript

as per manufacturer instructions (Stratagene, Cambridge, UK). All samples were incubated 55 ^{o}C

for 60 minutes and 70 ^{o}C for 15 minutes with the exception of random primers, which were pre

incubated at 25 ^{o}C for 10 minutes. Synthesised cDNA was then stored at -20°C until required.

Oligonucleotides were designed using MacVector™ (Oxford, Biomolecular, UK) and synthesized

409   commercially by Life Technologies Ltd. (Paisley, UK). All standard PCR amplification reactions

410   were performed in 25µl reactions. Each reaction contained 1µl 10X High Fidelity PCR Buffer, 1µl

411   10 mM dNTP mixture, 1µl 50 mM $MgSO_4$, 25 pmol forward and reverse oligonucleotide primers,

412   18µl molecular H_2O, and 1µl of *A. castellanii* cDNA or gDNA. The samples were then incubated at

413   94 ^{o}C for 1 minute before the addition of 0.5µl Platinum® Taq High Fidelity (Life Technologies).

414   25pmol forward and reverse oligonucleotide primers, 10.5µl molecular H_2O (Life Technologies),

415   1µl of *A. castellanii* cDNA or gDNA. The reactions were performed with initial denaturing at 95°C

416   for 3-5 minutes followed by 35 or 40 cycles of denaturing at 95 ^{o}C for 30 seconds, annealing at 52

417   ^{o}C-64 ^{o}C for 45 seconds and extension at 72 ^{o}C for 1-2 minutes. These reactions were then

418   completed with a final extension at 72 ^{o}C for 10 minutes. PCR products were visualised in a 0.8 -

419   2% agarose gel on a transilluminator following ethidium bromide staining.

Cloning and sequencing of PCR products: PCR-amplified DNA fragments were isolated from ethidium bromide stained agarose gels via MinElute Gel Extraction Kit (Qiagen, Crawley, United Kingdom). The purified PCR amplified products were ligated into the pDRIVE vector using the Qiagen PCR Cloning Kit (Qiagen) according to the manufacturer's instructions. Competent DH5α were transformed with 5µl of the ligation reaction using the heat shock method (Cohen et al. 1972). Transformed cells were then spread evenly onto LB agar (Sigma, Poole, United Kingdom), which had been previously coated with 100µg/ml ampicillin, 500µM/ml IPTG and 50µg/ml X-gal (Sigma, Poole, United Kingdom) and incubated overnight at 37 °C. Successful transformants were screened by blue/white screening and plasmid purification using the QIAprep Spin Miniprep Kit (Qiagen) according to the manufacturer's instructions. Restriction enzyme digest with EcoR1 Digested fragments were assessed via agarose gel electrophoresis. Automated sequencing of PCR amplified products was achieved using the M13 forward and reverse primers and performed commercially by Geneservice Ltd., Cambridge, UK or GATC in accordance with company guidelines. Sequences were then assembled using Sequencher^{TM} 4.0 (GeneCodes, USA).

Modelling: Modelling of the *A. castellanii* shikimate pathway proteins was done using the Phyre2 server (Kelley and Sternberg 2009) and proposed ligand binding sites detected using the 3DLigand server (Wass et al. 2010).

Acknowledgements

References

444

Ahn HJ, Yoon HJ, Lee B 2nd, Suh SW (2004) Crystal structure of chorismate synthase: a novel

445

FMN-binding protein fold and functional insights. J Mol Biol **336**:903-915

446

447

Bentley R (1990) The shikimate pathway--a metabolic tree with many branches. Crit Rev Biochem

448

Mol Biol **25**:307-384

449

450

Butler, JR, Alworth, WL, Nugent, MJ (1974) Mechanism of dehydroquinase catalysed

451

dehydration 1. Formation of a shiff base intermediate. J Am Chem Soc **96**:1617-1618

452

453

Campbell SJ, Ingram PR, Roberts CW, Henriquez FL (2008) Induced encystment improves

454

resistance to preservation and storage of *Acanthamoeba castellanii*. Parasitology **135**:1401-1405

455

456

Campbell SA, Richards TA, Mui EJ, Samuel BU, Coggins JR, McLeod R, Roberts CW (2004)

457

A complete shikimate pathway in *Toxoplasma gondii*: an ancient eukaryotic innovation. Int J

458

Parasitol **34**:5-13

459

460

Chaleff RS (1974) The inducible quinate-shikimate catabolic pathway in *Neurospora crassa*:

461

induction and regulation of enzyme synthesis. J Gen Microbiol **81**:357-372

462

463

Chomczynski P, Sacchi N (1987) Single-step method of RNA isolation by acid guanidinium

464

thiocyanate-phenol-chloroform extraction. Anal Biochem **162**:156-159

465

466

Clarke M, Lohan AJ, Liu B, Lagkouvardos I, Roy S, Zafar N, Bertelli C, Schilde C,

467

Kianianmomeni A, Bürglin TR, Frech C, Turcotte B, Kopec KO, Synnott JM, Choo C,

468

Paponov I, Finkler A, Heng Tan CS, Hutchins AP, Weinmeier T, Rattei T, Chu JS, Gimenez

469

G, Irimia M, Rigden DJ, Fitzpatrick DA, Lorenzo-Morales J, Bateman A, Chiu CH, Tang P, Hegemann P, Fromm H, Raoult D, Greub G, Miranda-Saavedra D, Chen N, Nash P, Ginger ML, Horn M, Schaap P, Caler L, Loftus BJ (2013). Genome of *Acanthamoeba castellanii* highlights extensive lateral gene transfer and early evolution of tyrosine kinase signaling. Genome Biol. **14**:R11

Coggins JR, Duncan K, Anton IA, Boocock MR, Chaudhuri S, Lambert JM, Lewendon A, Millar G, Mousdale DM, Smith DD (1987). The anatomy of a multifunctional enzyme. Biochem Soc Trans **15**:754-759

Cohen SN, Chang AC, Hsu L (1972) Nonchromosomal antibiotic resistance in bacteria: genetic transformation of *Escherichia coli* by R-factor DNA. Proc Natl Acad Sci USA **69**:2110-2114

Dyer WE, Weaver LM, Zhao JM, Kuhn DN, Weller SC, Herrmann KM (1990) A cDNA encoding 3-deoxy-D-arabino-heptulosonate 7-phosphate synthase from *Solanum tuberosum* L. J Biol Chem. **265**:1608-1614

Ehammer H, Rauch G, Prem A, Kappes B, Macheroux P (2007) Conservation of NADPH utilization by chorismate synthase and its implications for the evolution of the shikimate pathway. Mol Microbiol **65**:1249-1257

Gosset G, Bonner CA, Jensen RA (2001) Microbial origin of plant-type 2-keto-3-deoxy-D-arabino-heptulosonate 7-phosphate synthases, exemplified by the chorismate- and tryptophan-regulated enzyme from *Xanthomonas campestris*. J Bacteriol **183**:4061-4070

Henriquez, FL, Ingram, PR, Muench SP, Rice DW, Roberts CW (2008) Molecular basis for resistance of *Acanthamoeba* tubulins to all major classes of antitubulin compounds. Antimicrob Agents Chemother **52**:1133-1135

Herrmann KM, Weaver LM (1999) The shikimate pathway. Annu Rev Plant Physiol Plant Mol Biol **50**:473-503

Jensen RA (1996) Tyrosine and phenylalanine biosynthesis: Relationship between alternative pathways, regulation and subcellular location. In Conn EE (ed), Recent Advances in Phytochemistry, vol. 20, The Shikimic Acid Pathway. Plenum Press, New York and London, pp 57–81

Jensen RA, Xie G, Calhoun DH, Bonner CA (2002) The correct phylogenetic relationship of KdsA (3-deoxy-d-manno-octulosonate 8-phosphate synthase) with one of two independently evolved classes of AroA (3-deoxy-d-arabino-heptulosonate 7-phosphate synthase). J Mol Evol **54**:416-423

Jiroutová K, Horák A, Bowler C, Oborník M (2007) Tryptophan biosynthesis in stramenopiles: eukaryotic winners in the diatom complex chloroplast. J Mol Evol **65**:496-511

Johnson AM, Dubey JP, Dame JB (1986) Purification and characterization of *Toxoplasma gondii* tachyzoite DNA. Aust J Exp Biol Med Sci **64**:351-355

Kelley LA, Sternberg MJ (2009) Protein structure prediction on the Web: a case study using the Phyre server. Nat Protoc **4**:363-371

Marciano-Cabral F, Cabral G (2003) *Acanthamoeba* spp. as agents of disease in humans. Clin Microbiol Rev **16**:273-307

McBride J, Ingram PR, Henriquez FL, Roberts CW (2005) Development of colorimetric microtiter plate assay for assessment of antimicrobials against *Acanthamoeba*. J Clin Microbiol **43**:629-634

McBride J, Mullen AB, Carter KC, Roberts CW (2007) Differential cytotoxicity of phospholipid analogues to pathogenic *Acanthamoeba* species and mammalian cells. J Antimicrob Chemother **60**:521-525

Richards TA, Dacks JB, Campbell SA, Blanchard JL, Foster PG, Mcleod R, Roberts CW (2006) Evolutionary origins of the eukaryotic shikimate pathway: gene fusions, horizontal gene transfer, and endosymbiotic replacements. Eukaryot Cell **5**:1517-1531

Roberts CW, Roberts F, Lyons RE, Kirisits MJ, Mui EJ, Finnerty J, Johnston JJ, Ferguson DJ, Coggins JR, Krell T, Coombs GH, Milhous WK, Kyle DE, Tzipori S, Barnwell J, Dame JB, Carlton J, McLeod R (2002) The shikimate pathway and its branches in apicomplexan parasites. J Infect Dis **185** Suppl 1:S25-S36

Roberts F, Roberts CW, Johnson JJ, Kyle DE, Krell T, Coggins, JR, Coombs GH, Milhous WK, Tzipori S, Ferguson DJ, Chakrabarti, D, McLeod R (1998). Evidence for the shikimate pathway in apicomplexan parasites. Nature **393**:801-805

Seijo Martinez M, Gonzalez-Mediero G, Santiago P, Rodriguez De Lope A, Diz J, Conde, C. Visvesvara GS (2000) Granulomatous amebic encephalitis in a patient with AIDS: Isolation of

23

547   *Acanthamoeba* sp. Group II from brain tissue and successful treatment with sulfadiazine and

548   fluconazole. J Clin Microbiol **38**:3892-3895

549

550   **Shukla OP, Kaul SM, Mehlotra RK** (1990) Nutritional studies on *Acanthamoeba culbertsoni* and

551   development of chemically defined medium. J Protozool **37**:237-242

552

553   **Shumilin IA, Kretsinger RH, Bauerle R** (1996) Purification, crystallization, and preliminary

554   crystallographic analysis of 3-deoxy-D-arabino-heptulosonate-7-phosphate synthase from

555   *Escherichia coli*. Proteins **24**:404-406

556

557   **Shumilin IA, Bauerle R, Wu J, Woodard RW, Kretsinger RH** (2004) Crystal structure of the

558   reaction complex of 3-deoxy-D-arabino-heptulosonate-7-phosphate synthase from *Thermotoga*

559   *maritima* refines the catalytic mechanism and indicates a new mechanism of allosteric regulation. J

560   Mol Biol **341**:455-466

561

562   **Walker GE, Dunbar B, Hunter IS, Nimmo HG, Coggins JR** (1996) Evidence for a novel class of

563   microbial 3-deoxy-D-arabino-heptulosonate-7-phosphate synthase in *Streptomyces coelicolor*

564   A3(2), *Streptomyces rimosus* and *Neurospora crassa*. Microbiology **142**:1973-1982

565

566   **Wass MN, Kelley LA, Sternberg MJ** (2010) 3DLigandSite: predicting ligand-binding sites using

567   similar structures. Nucleic Acids Res **38**: W469-W473

568

569   **Webby CJ, Jiao W, Hutton RD, Blackmore NJ, Baker HM, Jameson GB, Parker EJ** (2010)

570   Synergistic allostery, a sophisticated regulatory network for the control of aromatic amino acid

571   biosynthesis in *Mycobacterium tuberculosis*. J Biol Chem 285:30567-30576

24

Figure 1. Glyphosate restricts *A. castellanii* growth at concentrations which are not toxic to mammalian cells. The percentage of alamarBlue reduction was determined for *A. castellanii* Neff strain (**A**), Clinical strain (**B**) and RCE (**C**) by comparing test cultures to those of untreated controls. . Glyphosate significantly inhibited growth of the Neff strain, in a dose dependent manner from 17.5µM or above (p<0.05) (**A**). The IC$_{50}$ is between 17.5µM and 35µM. Glyphosate significantly inhibited growth of a Clinical isolate, from 17.5µM or above (p<0.05) (**B**). Glyphosate did not inhibit RCE growth (**C**). *A. castellanii* inhibited by glyphosate was washed in 5% SDS to determine cyst formation (D). 2.52 x10^5/ml cysts were found in the encystment media (C2). 8.52x10^3/ml cysts were counted in the untreated controls (C3). Glyphosate does not induce cyst formation. There is a, non-dose dependent, increase in the number of cysts in the presence of glyphosate to that of untreated controls. In the presence of glyphosate (280µM) 9.17x10^3/ml to (70µM) 1.25x10^4/ ml cysts were counted. The results are expressed as means for triplicate cultures ± SE.

Figure 2. Rescue assays were performed to determine specificity of glyphosate to EPSP synthase of the shikimate pathway. Rescue was determined by measuring the percentage alamarBlue reduction of test cultures compared to those of untreated controls. The addition of single aromatic amino acids (Phe, Trp and Tyr) did not ablate the effects of glyphosate (**A**). However, by adding either phenylalanine and tryptophan or all three amino acids together the effect of glyphosate is significantly diminished (p<0.0001 ***) (**B**). The presence of exogenous PABA did not rescue glyphosate inhibition of trophozoites (**C**).

Figure 3. Diagram of predicted phenylalanine and tyrosine biosynthesis in *A. castellanii* species. Enzymes highlighted in bold have been identified are present in Genbank. Pathways in grey are not present. (Chorismate mutase ELR23397, prephenate dehydratase ELR22681, aminotransferase ELR13846, phenylalanine-4-hydroxylase ELR14932, tyrosine aminotransferase ELR16760)

Figure 4. (**A**) Multiple sequence alignment of the two class I *A.castellanii* DAHP synthase sequences (AcDAHPIa, AcDAHPIb) and the *E. coli* DHAP synthase (EcDAHPI). Those residues conserved and similar are highlighted by red and blue boxes, respectively. Those residues involved in binding the Phe inhibitor are labelled by and F above the alignment. (**B**) Superposition of the EcDAHPI structure (yellow) and AcDAHPIa model structure (Magenta). Those residues which form the Phe binding site

are shown in stick format and coloured yellow, red, and blue for carbon, oxygen and nitrogen, respectively. (**C**) Surface view of the Phe binding site from EcDAHPI. (**D**) Surface view of the EcDAHPI structure with the Ser/Gly mutation as seen in the AcDAHPIb sequence which produces an increase in space for the bound Tyr residue shown in stick format.

Figure 5. (**A**) Multiple sequence alignment of the AcDAHPII and MtDAHPII enzymes with those residues conserved and similar highlighted by red and blue boxes, respectively. Those residues involved in binding an amino acid inhibitor are shown by the label F1 (Primary Phe binding site), F2 (Secondary Phe binding site) and W (Trp binding site). The primary Phe binding site (**B**) and Trp binding site (**C**) in MtDAHPIIwith the AcDAHPIImodel structure superposed. The MtDAHPII structure is shown in yellow and AcDAHPII magenta. Those residues which have been shown to play a role in binding are shown in stick format and coloured Yellow (MtDH2) or Magenta (AcDAHPII) for carbon, red for oxygen and blue for nitrogen. The Lys residue which has been proposed to stabilise the α-carboxylate group of the Trp inhibitor in MtDAHPII is highlighted by a star (C).

Figure 6. Arrangement of the shikimate pathway enzymes. In Bacteria and plants DAHP synthase (**red**), 3-dehydroquinate synthase (**orange**), 5-enolpyruvylshikimate-3-phosphate synthase (**purple**), shikimate kinase (**blue**), 3-dehydroquinate dehydratase (**yellow**), shikimate 5-dehydrogenase (**green**) and chorismate synthase (**pink**) are encoded on individual polypeptides. In plants, 3-dehydroquinate dehydratase and shikimate 5-dehydrogenase are found on separate domains of the same polypeptide. Plant enzymes have n-terminal transit sequences that target the enzymes to the chloroplast. In fungi, alveolates and oomycetes, 3-dehydroquinate synthase, 3-dehydroquinate dehydratase, shikimate 5-dehydrogenase, shikimate kinase and EPSP synthase are encoded on a single transcript to form a pentafunctional polypeptide (AROM). Two evolutionary unrelated forms of DAHP synthase have been found and designated DAHP synthase I and DAHP synthase II. Bacteria such as *E. coli* have 3 isoenzymes of DAHP synthase I, but plants such as *Arabidopsis thaliana* and the apicomplexan *T. gondii* have a single DAHP synthase II. Certain fungi including *N. crassa* have 2 isoenzymes of DAHP synthase I and a DAHP synthase II.   In *A. castellanii*, 3-dehydroquinate synthase, 3-dehydroquinate dehydratase, shikimate 5-dehydrogenase, shikimate kinase and EPSP synthase are part of a tetra-functional polypeptide (ARON). DAHP synthase and chorismate synthase are found as individual polypeptides. *A. castellanii*, has 2 isoenzymes of DAHP synthase I and a

26

DAHP synthase II. Shikimate 5-dehydrogenase is found fused to PRAI-IGPS, an arrangement that is not found in any other organism to date.

Supplementary Figures

Figure S1. Enzymes involved in the folate and tryptophan pathways are present in the *A. castellanii* transcriptome[26]

Figure S2. Multiple alignment of AROMn with other known AROM sequences from fungal species

Figure S3. Multiple alignment of *A.castellanii* IGPS-SD with other fungal species. The tri-protein fusion of IGPS-SD in *Acanthamoeba* is novel in nature

Figure S4. Multiple alignment of *A. castellanii* chorismate synthase with other fungal species
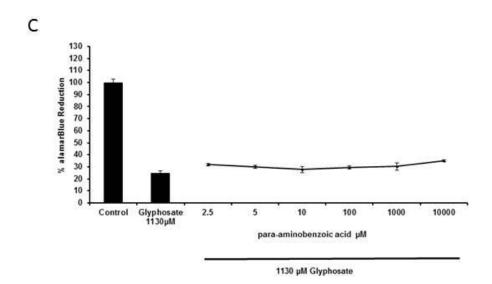
Figure 1

Figure 2

Figure 2

Phenylalanine and Tyrosine synthesis

CHORISMATE

CHORISMATE MUTASE

PREPHENATE

		PREPHENATE DEHYDROGENASE
PREPHENATE DEHYDRATASE	PREPHENATE AMINOTRANSFERASE	

PHENYLPYRUVATE **AROGENATE** 4-HYDROXYPHENYLPYRUVATE

AMINOTRANSFERASE AMINOTRANSFERASE

AROGENATE DEHYDRATASE AROGENATE DEHYDROGENASE

PHENYLALANINE **TYROSINE**

PHENYLALANINE-4-HYDROXYLASE

Figure 3

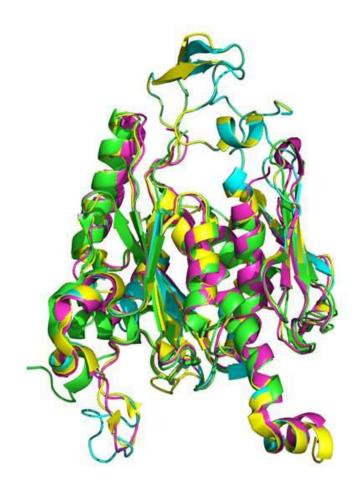Figure 4

Figure 5

Figure6

Figure 7

Chorismate

    ⬇   Para-amino benzoate synthase 2.6.1.85 **(ELR22073.1)**

Aminodeoxychorismate

    ⬇   Deoxychorismate lyase 4.1.3.38

P-aminobenzoate

    ⬇   Hydroxymethyldihydropteridine diphosphokinase 2.7.6.3* **(AFW17812.1)**

2-amino-4-hydroxy-6-hydroxymethyl 7,8-dihydropteridine-p2

    ⬇   Dihydropteroate synthase 2.5.1.15* **(AFW17812.1)**

Dihydropteroate

    ⬇   Dihydrofolate synthase 6.3.2.17 **(ELR15504.1/ELR22074.1)**

Dihydrofolate

    ⬇   Dihydrofolate reductase 1.5.1.3** **(XP_004341781)**

Tetrahydrofolate

trifunctional gene product with dihydroneopterin aldolase
**Bifunctional gene product with thymilidate synthase*

Chorismate

    ⬇   Anthranilate synthase 4.1.3.27 **(ELR21148.1)**

Anthranilate

    ⬇   Anthranilate phosphoribosyltransferase 2.4.2.18 **(XP_004344889)**

N-(5'phosphoribosyl) anthranilate

    ⬇   N-(5'phosphoribosyl) anthranilate isomerase 5.3.1.24* **(AGK89943)**

Enol-1-0 carboxyphenylamino-1-deoxyribulose phosphate

    ⬇   Indole-3-glycerolphosphate synthase 4.1.1.48* **(AGK89943)**

Indole-3-glycerol phosphate

    ⬇   Tryptophan synthase 4.2.1.20 **(XP_004344892)**

Tryptophan

*trifunctional gene product indole-3-glycerol phosphate synthase,
phosphoribosylanthranilate isomerase and shikimate dehydrogenase*

Figure S1

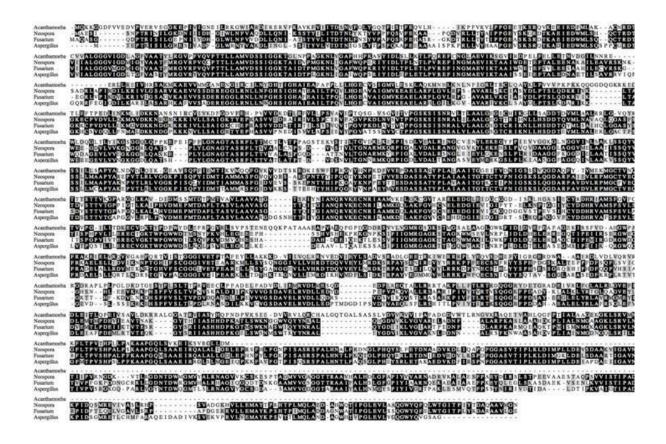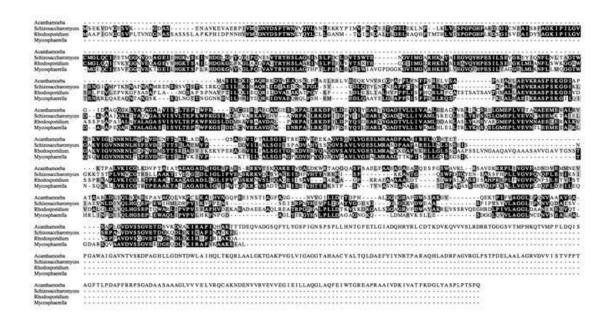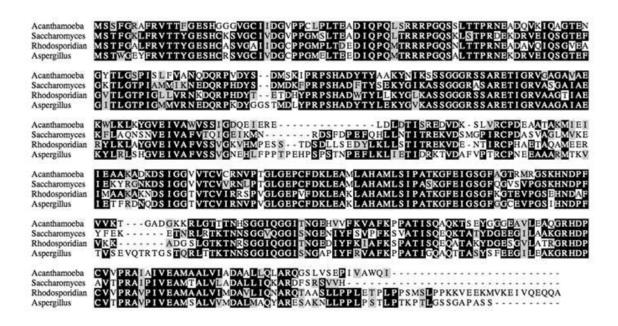Figure S2

Acanthamoeba
Schizosaccharomyces
Rhodosporidium
Mycosphaerella

Figure S3

Figure S4